Journal of Volcanology and Geothermal Research 203 (2011) 168–174

Contents lists available at ScienceDirect

Journal of Volcanology and Geothermal Research

journal homepage: www.elsevier.com/locate/jvolgeores

Short communication

# The porosity of pyroclasts as an indicator of volcanic explosivity

Sebastian Mueller [a,b,*], Bettina Scheu [b], Ulrich Kueppers [b], Oliver Spieler [b], Dominique Richard [b], Donald B. Dingwell [b]

[a] School of Earth Sciences, University of Bristol, Wills Memorial Building, Queens Road, Bristol BS81RJ, United Kingdom
[b] Earth and Environmental Sciences, Ludwig-Maximilians Universität, Theresienstr. 41, 80333 Munich, Germany

ARTICLE INFO

*Article history:*
Received 29 April 2010
Accepted 10 April 2011
Available online 17 April 2011

*Keywords:*
magma porosity
porosity distribution histogram
eruption styles
Volcanic Explosivity Index
field density measurements

ABSTRACT

The porosity of pyroclasts is a valuable indicator of the character of a volcanic eruption. Here, we analyse the porosity distribution of deposits of 17 different volcanic eruptions, covering a broad range of inferred magma properties and observed eruption styles. Histograms of porosity versus pyroclast frequency show distinctive features in terms of the mean, variance, modality, and skewness. We present characteristic porosity distributions for five different eruption-style categories: dome-forming, explosive basaltic, cryptodome forming, Subplinian/Plinian/Ultraplinian, and phreatomagmatic. We find that the mean porosity values of the deposits correlate positively with the Volcanic Explosivity Index (VEI) of Newhall and Self (1982), regardless of the degree of complexity of the individual distributions. We then propose causes of the deviations from a general trend in terms of magma viscosity, degassing efficiency, and cap-rock confinement. Finally, a generalised correlation between clast porosity and explosivity of an eruption is developed that should help, together with conventional field techniques, facilitate the interpretation of pyroclastic sequences, even in cases where no direct observation of the eruption exists.



## 1. Introduction

The porosity of magma influences magma properties and thus volcanic processes in many ways that determine eruptive style (e.g. rheology; Llewellin et al., 2002, thermal conductivity; Bagdassarov and Dingwell, 1994, permeability; Mueller et al., 2005, fragmentation threshold; Alidibirov and Dingwell, 1996; Spieler et al., 2004). As magma rises from depth and the flow pressure drops, volatiles in the magma become oversaturated, ultimately leading to bubble nucleation and growth. These bubbles (the 'vesicularity') define, together with pre-, syn-, and post-eruptive fractures, a magma's porosity. The volume percentage of bubbles and the acting pressure, achieved by diffusion of oversaturated volatiles during nucleation and bubble growth, have tremendous influence on the reaction of this complex system to both slow and rapid changes in deformation rate, decompression, and cooling.

The character and explosive potential of a volcanic eruption is determined by a wide range of interacting physical and chemical properties. However, a key role in this respect falls to the interplay between the three factors gas overpressure, pore volume fraction, and magma viscosity. Gas overpressure is considered to be the main energy source driving fragmentation, whereas the total pore volume (i.e. the porosity) determines the total amount of overpressure that can be stored in a magma (accordingly, the product of pore volume fraction and overpressure defines the "energy density" of a magma; e.g., Mueller et al., 2008). The magma viscosity may sustain the overpressure, and determines in which manner the expanding force of the overpressure is dissipated (i.e. fragmentation or bubble growth). In this study, we focus on the role of magma porosity.

There is abundant evidence that dense, low-porosity magma (either due to low initial volatile contents, phase separation in low-viscous systems, or permeable degassing) is typically associated with low-explosivity or effusive eruptions, whereas gas rich, vesicular magma often leads to highly energetic explosions. As a link between the porosity of magma and the dynamics of a specific eruption is evident, it can be expected that the porosity distribution of erupted pyroclasts may be a significant source of information from which to constrain conduit dynamics and eruptive style. Together with the evaluation of deposit characteristics (as e.g. area of distribution, deposit thickness), the investigation of the porosity distribution of primary volcanic deposits, sufficiently well-documented, should contribute to an enhanced understanding and modelling of eruption physics. It may also help to reconstruct, in a qualitative way, the eruptive character from deposits eruptions that lack recorded observations.

Direct observation of volcanic conduit rocks is restricted to the investigation of eroded edifices (which, due to their age, are often highly chemically and physically altered), or to drilling projects (which can present major technical and financial challenges). There is at present disagreement as to whether the conduit-filling rocks of the final stages of an eruption are representative of the magma that was

* Corresponding author at: School of Earth Sciences, University of Bristol, Wills Memorial Building, Queens Road, Bristol BS81RJ, United Kingdom.
*E-mail address:* s.mueller@bristol.ac.uk (S. Mueller).

0377-0273/$ – see front matter © 2011 Elsevier B.V. All rights reserved.
doi:10.1016/j.jvolgeores.2011.04.006

rising through the conduit at earlier stages. Assuming that the physical and textural properties of high-viscosity, silica-rich magma are subject to only minor changes after fragmentation, information on the spatial and temporal variability of the ascending magma's porosity can be most easily achieved via the measurement of a statistically reliable number of representative pyroclasts (Houghton and Wilson, 1989; Kueppers et al., 2005).

Here we compare the porosity distributions of deposits of 17 volcanic eruptions, covering a broad range in magma chemistry and eruptive styles. The data set generated is novel in both range and precision. In the following section, we give a short overview of the eruptions analysed and the methods used. In Section 3 we categorize the eruptions according to the main characteristics of their porosity distribution, and in Section 4 we link the mean porosity values of the deposits to the style and explosivity index of the corresponding eruptions.

## 2. Investigated eruptions and measurement techniques

For this study we have measured the porosity distribution of deposits of seven volcanic eruptions: Augustine 1986 (USA); Bezymianny 1956 (Russia); Merapi 1998; Kelut 1990; Krakatau 1883; Anak Krakatau 1999 (all Indonesia); and Colima 1998–2005 (Mexico). Furthermore, we have compiled 10 datasets from literature, in order to augment the database and to compare to our data. The compiled datasets include porosity distribution histograms of Unzen 1990–95 (Japan, Kueppers et al., 2005); Mt. St Helens 1980 (USA, Hoblitt and Harmon, 1993); Novarupta 1912 (USA, Adams et al., 2006); Campanian Ignimbrite 37,000 yBP (Italy, Polacci et al., 2003); Taupo 1800 yBP (New Zealand); Kilauea Iki 1959 (USA, both Houghton and Wilson, 1989); Stromboli 2002 (Italy, Lautze and Houghton, 2008); Karymskoye lake 1996 (Russia, Belousov and Belousova, 2001); Crater Hill (New Zealand, Houghton et al., 1996); and Rotokawau 3400 yBP (New Zealand, Houghton and Smith, 1993).

For a summary of the main characteristics of these 17 eruptions, see Table 1. A more detailed description of the eruptions and the samples analysed can be found as online supplement.

In our field campaigns we determined the porosity of pyroclasts following the method described in (Kueppers et al. 2005): the density of a pyroclast is hereby determined by first weighing the sample in air, and subsequently under water ('Archimedean principle'). Water infiltration is prevented by an evacuated plastic bag, which tightly covers the sample surface. The clast bulk density is then calculated according to $\rho_{sample} = (m_{air}/(m_{air} - m_{water}))\rho_{water}$, with $m_{air}$ being the mass of the sample evacuated in a plastic bag in air and $m_{water}$ being the mass of the same sample submerged. For the calculation, $\rho_{water}$ was assumed to be 1. In order to determine the clast's porosity, one needs to know also its matrix density $\rho_{matrix}$ (or 'dense rock equivalent', DRE). Representative matrix density values for each sample type have been determined by measuring powdered samples in a He–Pycnometer in the laboratory. The samples' porosity $\Phi$ (in %) is then calculated as follows:

$$\Phi = 100\left(\rho_{matrix} - \rho_{sample}\right) / \rho_{matrix}. \quad (1)$$

The density data compiled from literature were mostly measured according to the method described by (Houghton and Wilson, 1989).

## 3. Interpreting volcanic porosity distributions

### 3.1. Magma vesicularity and fragmentation

During rise, the physical and chemical conditions in magma change, giving rise to both crystal and bubble growth (e.g., Sparks, 1978, Cashman et al., 2000). Together with fractures, these bubbles dominate the magma porosity (note that fractures have, by their nature, a very small volume, so we here consider their contribution to total porosity negligible). The resulting porosity distribution of the erupted pyroclastic deposits thus depends on the vesiculation history of the magma and the nature of the process terminating the vesiculation. According to Houghton and Wilson (1989) the latter could be (1) non-explosive degassing, (2) magmatic fragmentation, or (3) interaction of the magma with external water (phreatomagmatic fragmentation).

*Non-explosive degassing* can occur either through buoyant bubble rise, if the viscosity of the magma is low enough, or through a permeable network of interconnected pores, leading to collapse of magma pores at depth (e.g., Eichelberger et al., 1986, Mueller et al., 2005). This mechanism is important in dome-forming eruptions and generally leads to effusive products of low porosity.

One can distinguish two main mechanisms leading to *magmatic fragmentation*. Firstly, the bubbles in a rising magma grow to the point that they start to interfere, leading to rupture of the inter-bubble melt films (Sparks 1978). In this case the fragmentation threshold (or

**Table 1**
Main characteristics of the volcanic deposits analysed and compared in this study; baf = block-and-ash-flow (dome collapse), spl = Subplinian, pl = Plinian, upl = Ultraplinian, db = directed blast (sector collapse), phm = phreatomagmatic, haw = Hawaiian (lava fountaining), str = Strombolian. VEI classifications from Siebert and Simkin (2002).

| Volcano | Eruption | Eruption type | VEI | Rock type | DRE (g/cm$^3$) | Data Source |
|---|---|---|---|---|---|---|
| Augustine | 1986 | spl | 4 | Andesite | 2.64 | This study |
| Bezymianny | 1956 | db, pl | 5 | Andesite | 2.67 | This study |
| Colima | 1998–2005 | baf | 2–3 | Andesite | 2.73 | This study |
| Krakatau | 1883 | pl | 6 | (Rhyo) dacite | 2.47 | This study |
| Anak Krakatau | 1999 | str | 2 | Basaltic andesite | 2.83 | This study |
| Kelut | 1990 | spl | 4 | Basaltic andesite | 2.76 | This study |
| Merapi | 1998 | baf | 2 | Basaltic andesite | 2.82 | This study |
| Unzen | 1990–95 | baf | 1 | Dacite | 2.60 | Kueppers et al. 2005 |
| St Helens | 1980 | db, pl | 4–5[a] | Dacite | 2.69[b] | Hoblitt and Harmon 1993 |
| Stromboli | 2002 | str | 2 | Basalt | 2.75 | Lautze and Houghton 2008 |
| Crater Hill | Late quaternary | phm | 2–3 [c] | Basalt | 3.00 | Houghton et al. 1996 |
| Rotokawau | 3400 yBP | phm | 2–3[c] | Basalt | 2.80[c] | Houghton and Smith, 1993 |
| Karymskoye lake | 1996 | phm | 3 | Basalt | 2.80 | Belousov and Belousova, 2001 |
| Novarupta | 1912 | pl | 6 | Dacite-Rhyolite | 2.45 | Adams et al. 2006 |
| Taupo | 1800 yBP | upl | 7 | Rhyolite | 2.40 | Houghton and Wilson 1989 |
| Kilauea Iki | 1959 | haw | 2 | Basalt | 2.90 | Houghton and Wilson 1989 |
| Camp. Ignimbrite | 37,000 yBP | (u)pl | 6 | Trachyte | 2.41 | Polacci et al. 2003 |

[a] Explanation see text.
[b] Own DRE measurement.
[c] Estimated.

criterion) is a fixed value, or range, of porosity, depending on the degree of bubble deformation and polydispersity (e.g., monodisperse spherical bubbles can start to fully interact at ~52% porosity, whereas highly polydisperse and deformed bubbles can result in froths with a porosity of >95%). This fragmentation mechanism is considered to be important in sustained, steady eruption types (Subplinian and Plinian) and in low-viscosity magma eruptions (basaltic fire fountaining). The expected porosity distribution of the erupted pyroclasts in this case is unimodal and, due to the porosity-controlled fragmentation criterion, narrow (low variance), with a generally high mean value. Secondly, magma can fragment in a more transient manner if bubble overpressure due to volatile exsolution and/or decompression of the entire vesicular magma (e.g., Vulcanian eruptions, sector collapse) exceeds the strength of the magma (Fowler et al., 2010). In this case the fragmentation threshold is a function of not only magma porosity, but also of the decompression characteristics (pressure differential and decompression rate; Spieler et al., 2004) and the amount of overpressure lost by permeable degassing (Mueller et al., 2008). The resulting porosity distribution can be expected to be broad with a high variance (see Section 3.2).

In the case of *phreatomagmatic fragmentation*, the magma interacts with external water and thus the eruptive energy derives from the degree of magmatic volatiles exsolution and the rate of steam production through evaporation in a confined volume. The resulting porosity profile will strongly depend on the type and ascent history of the magma, as well as on the depth of the magma–water interaction. In general, a broad distribution can be expected due to the heterogeneous nature of the deposited clasts (juvenile and lithics). The mean porosity of phreatomagmatic deposits is expected to be comparatively low, because vesiculation of the clasts is often hindered due to rapid quenching by water contact. Additionally, much of the eruptive energy in such eruptions is provided by steam flashing due to magma–water contact, allowing for even relatively dense magma to be explosively ejected.

### 3.2. A phenomenological review of porosity distribution patterns

Generally, a porosity vs. clast number (or frequency) distribution can show variations in the following statistical parameters (Fig. 1):

(a) The position of the curve on the porosity spectrum can be expressed by the value of the curve's peak (the numeric value with the highest frequency), its mean (average value) or its median (numeric value separating the higher half of a distribution from the lower half). The curve's position reflects the volatile content of the magma, the degree of gas exsolution at the time of eruption, and the efficiency of gas loss to the atmosphere before eruption. External influences such as magma-water interactions may distort the original distribution.

(b) The variance is a measure of the statistical dispersion, and indicates how broad a distribution is; commonly it is expressed as the square of the standard deviation, $\sigma^2$. The variance of a porosity distribution mainly reflects the type of fragmentation. Bubble interaction and rupture in sustained eruptions will occur at a defined threshold of porosity, resulting in a narrow porosity distribution (Houghton and Wilson, 1989). In contrast, "decompressive" fragmentation affects and erupts magma from various depths and with a much wider range of porosity, because once the pressure differential required for fragmentation is met for a certain porosity, fragmentation will also occur in magma of higher porosity. Dense magma batches and enclaves as well as parts of the wall rock are likely to be ruptured and incorporated in the violent ejection of pyroclasts. Pumices, on the other hand, can continue to vesiculate during or after ejection. The result will be a broad porosity distribution with a high variance. This statement also holds for phreatomagmatic fragmentation; once triggered, it will affect magma and country rock irrespective of porosity or pressurization state.

(c) If two or more types of magma with clearly different physicochemical properties or vesiculation and degassing histories are involved in a single eruption, the resulting porosity distribution will likely show a bi- or multi-modal pattern. Such distinctions have been interpreted as the result of different nucleation events in spatially separated batches of magma (Hoblitt and Harmon, 1993), or of the mixture of juvenile clasts (high porosity) and degassed dome material (low porosity; e.g., Belousov et al., 2007) intermingled during an explosive eruption.

(d) Porosity distributions can be asymmetric (skewed) and show tails in either direction. The relative position of the mean (*mn*) and median (*md*) values of the distribution gives information about the orientation of the skewness: if $mn > md$ the long tail is at high values ("positive skew"); if $mn < md$: the long tail is at low values ("negative skew"). Because the porosity of pyroclasts is usually confined towards one end of the porosity scale, most distributions are skewed. In negatively skewed distributions the porosity is capped towards high values by the fragmentation criterion (see Section 3.1). Entrainment of degassed material causes a relatively long tail at the low porosity end. In contrast, at volcanoes with generally low porosity magma, positively skewed distributions are more common. Eruptions are likely to be triggered by dome destabilization and collapse, leading to block-and-ash flows. Occasional explosive components with higher vesicle content (e.g. breadcrust bombs) are the reason for a tail at the high-porosity end.

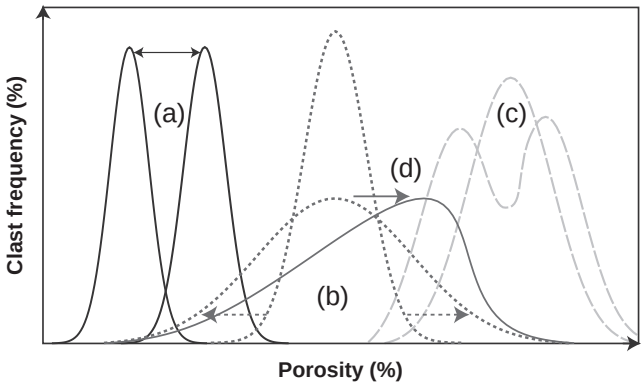


**Fig. 1.** Schematic variations of porosity distribution curves: (a) general position of the curve; (b) spread of the distribution, reflected by a different variance and standard deviation; (c) modality of the distribution (uni-, bi-, or multi-modal); (d) skewness or symmetry of the curve (negative skew in this example).

### 3.3. Comparison of volcanic porosity distributions

When investigating physical aspects of explosive eruption and fragmentation mechanisms, the porosity of the erupting magma is more relevant than its bulk density. We therefore convert all pyroclast density data, measured or taken from literature, into porosity data, using Eq. (1). For that, the corresponding matrix density (DRE) must be known. For comparison, in the online supplement we present the respective raw density distributions of all 17 eruptions investigated here.

The statistical parameters of the distributions, such as mean porosity, variance, and median are given in Table 2. In order to depict similarities and correlations in their porosity distributions, we group the data of the 17 eruptions according to their known eruptive style

**Table 2**
Values of the mean porosity, the variance $\sigma^2$, and the median of the investigated porosity distributions. The comparison of mean and median values defines the orientation of the skew.

| Eruption | Mean ϕ (%) | Variance $\sigma^2$ | Median Φ (%) | Skew |
|---|---|---|---|---|
| Augustine 1986 | 61.4 | 187.69 | 61.3 | ± |
| Bezymianny 1956 | 32.4 | 106.09 | 34.5 | ± |
| Colima 1998–2005 | 16.4 | 94.09 | 14.9 | + |
| Krakatau 1883 | 76.9 | 44.89 | 77.8 | ± |
| Anak Krakatau 1999 | 52.1 | 126.96 | 55.4 | − |
| Kelut 1990 | 65.78 | 56.07 | 66.0 | ± |
| Merapi 1998 | 26.2 | 72.25 | 25.4 | + |
| Unzen 1990–95 | 23.2 | 82.81 | 22.2 | + |
| St Helens 1980 | 32.4 | 158.76 | 33.5 | − |
| Stromboli 2002 | 61.5 | 43.56 | 60.4 | ± |
| Crater Hill | 34.9 | 63.20 | 33.5 | + |
| Rotokawau | 31.5 | 58.27 | 30.1 | + |
| Karymskoye lake | 33.4 | 101.56 | 30.0 | + |
| Novarupta 1912 | 68.5 | 37.21 | 67.3 | ± |
| Taupo 1800 yBP | 72.1 | 16.81 | 69.8 | + |
| Kilauea Iki 1959 | 73.4 | 56.52 | 70.4 | + |
| Campanian Ignimbrite 37,000 yBP | 75.9 | 53.29 | 72.6 | + |

(Fig. 2), and interpret the distributions on the basis of the criteria described in Section 3.2:

(a) Dome extrusion and block-and-ash flows: dome forming eruptions with occasional explosions, but dominated by gravitationally driven block-and-ash flow activity (VEI 1–3). The mean porosity is generally low (below 30%) and the distributions are rather broad. A more or less pronounced bimodality of the curve indicates a blend of more than one degassing stage within the deposits (e.g., juvenile material and older cap rock). The distributions commonly show positive skew.

(b) Explosive basaltic: gas-rich, Hawaiian or Strombolian eruptions of low-viscosity magma. The porosity distributions show peaks at 60–70%, consistent with the theory for magmatic fragmentation of low viscosity magma (Houghton and Wilson, 1989). The variance is intermediate to low, and the distributions are predominantly unimodal, with no explicit skewness. The explosivity of these eruptions is commonly low (VEI 1–2).

(c) Cryptodome and lateral blast: cryptodome formation followed by a sector-collapse-induced lateral blast (VEI 4–5). Bezymianny 1956 and Mount St. Helens 1980 eruptions are two examples of such eruptions with preceding cryptodome growth. The mean porosity value is around 30% for both deposits. This rather low value compared to the degree of explosivity likely reflects the fact that vesiculation in a cryptodome environment was suppressed due to high lithostatic pressure. The clearly bimodal porosity has been interpreted as the result of a non-uniform degassing of an initially homogenous batch of magma (Hoblitt and Harmon, 1993). Entrainment of accidental (non-juvenile) clasts during the blast might as well alter the distribution.

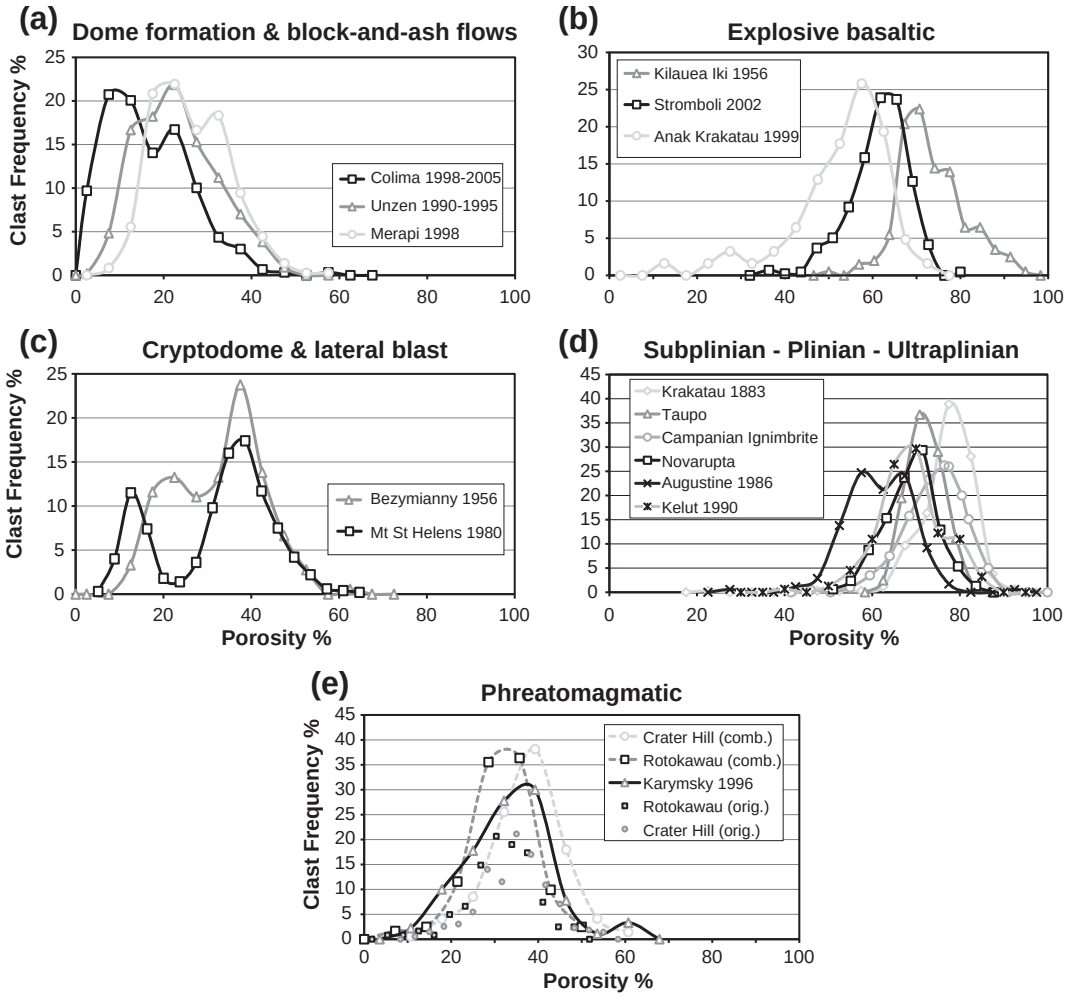


**Fig. 2.** Porosity distributions of 17 eruptions, grouped according to their fragmentation behaviour and eruptive style (a)–(e). Note: at (e) the porosity steps of the different distributions vary. For better comparison the data were averaged to the coarsest distribution (Karymsky Lake 1996). The original porosity data are plotted as small circles/rectangles.

(d) Subplinian, plinian and ultraplinian: highly explosive eruptions with Plinian phases (VEI 4–7). The deposits of these eruptions derive from fall-out or pyroclastic density currents. Fall-out deposits show almost perfect Gaussian distributions with a high mean porosity at 70–80%, those of the pyroclastic density currents are somewhat more irregular, but still unimodal with a mean porosity at 60–80%. The variance of the fall out distributions is in general narrower than for the pyroclastic density currents.
Note that both groups where pyroclasts are generated by 'dry' magmatic fragmentation (explosive basaltic and Subplinian to Ultraplinian eruptions) show similar distributions patterns in terms of mean porosity, variance and modality, despite their differences in, e.g., magma viscosity.

(e) Phreatomagmatic: explosive eruptions triggered by magma-water interaction (VEI 2–3). The porosity distributions are unimodal with no apparent skewness. Indicative for phreato-magmatic distributions are comparatively low mean porosity values of 30–35%, and a rather broad variance.

## 4. The correlation between porosity and volcanic explosivity

The Volcanic Explosivity Index (or VEI) was introduced by Newhall and Self (1982) as a measure of the size of an explosive volcanic eruption. It is a semi-quantitative logarithmic scale and is based on a combination of erupted tephra volume, eruption plume height and a subjective description by observers. The VEI ranges from 0 ("non-explosive") to 8 ("colossal"). A VEI 6 eruption, for example, corresponds to an erupted bulk tephra volume of 10–100 $km^3$ (Newhall and Self, 1982, Siebert and Simkin, 2002, Mason et al., 2004).

As outlined in Section 3.1, the explosive potential of a volcano is subtly related to the porosity of the magma. We therefore compare the mean porosity values of clasts from the 17 eruptions classified in Section 3.2 with the respective VEI (Fig. 3). The plot can be interpreted as a positive main trend between VEI and mean porosity (1) with deviations in both directions (2 and 3).

A general positive relationship between porosity and explosivity is not surprising, because –as outlined above – a higher porosity means more stored pressurized gas in the magma, and more energy available for magma fragmentation and particle ejection. As the porosity of a pyroclast is naturally confined, and the erupted volume (and, accordingly, the VEI) is – at least theoretically – unlimited, the general trend can be expected to show a positive gradient with an asymptotic behaviour towards $\Phi = 100\%$.

Explosive basaltic eruptions deviate from the main trend towards low explosivity (2). Hawaiian and Strombolian eruptions of basalts are characterized by a comparatively low magma viscosity, which often allows the bubbles to rise faster than the magma, with the according loss of potential explosive energy. The low magma viscosity further hinders the build up of significant overpressure in vesicles, as it facilitates pressure dissipation through bubble expansion. In combination, this leads to a low degree of explosivity at a comparatively high volatile content and porosity. Given the fact that the eruptions analysed in this study probably represent high porosity end-member examples for basaltic explosions, the field for this type of deviation likely extends towards lower porosities.

The cryptodome-forming eruptions of Bezymianny and Mount St. Helens deviate from the general trend towards higher VEI scales (3). This behaviour can be explained by a slow rise or a prolonged residence of the magma inside the volcanic edifice. In contrast to the depressurization history of a normal dome-forming magma, the higher lithostatic pressure within a cryptodome suppresses volatile exsolution and bubble expansion (and thus porosity development). The bubbles that do grow, however, are highly pressurized with respect to the lithostatic pressure. Gas loss in such a system can be expected to be low because (i) bubble rise is hindered by the comparatively high magma viscosity, (ii) the moderate porosity suppresses the development of a permeable network, and (iii) the low-permeability cap hinders degassing to the atmosphere. Together with the massive scale of decompression accompanying the eruption-triggering sector collapse and consequent exposure of the highly pressurized underlying magma, this results in highly explosive events in comparison to the moderate magma porosity. The comparatively high magma viscosity together with the imminent response to a rapid decompression allows only minor late stage bubble nucleation and growth, so that a porosity distribution clearly distinctive from effusive dome-forming eruptions is preserved.

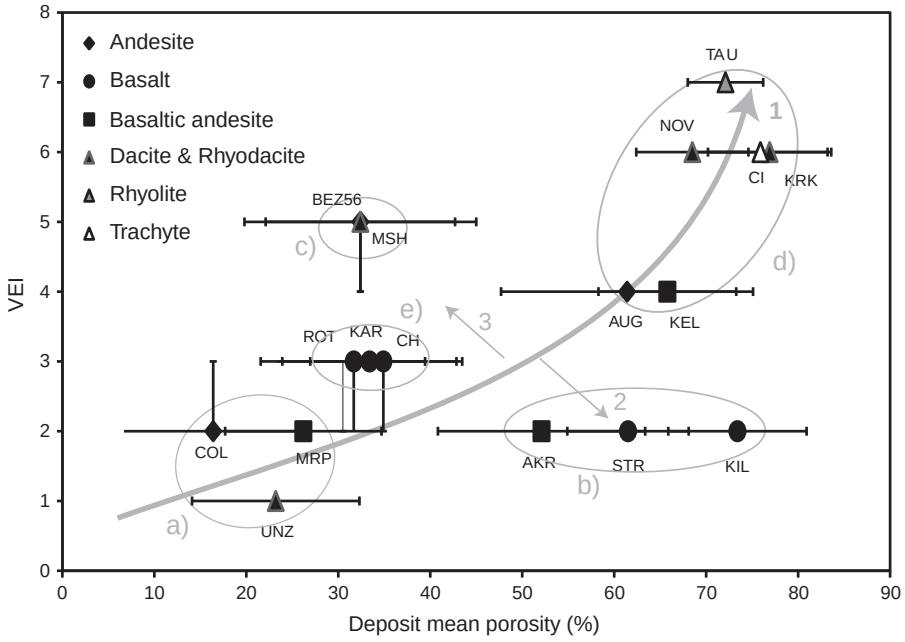


**Fig. 3.** Correlation between mean deposit porosity and volcanic explosivity index (VEI) of the respective eruption. Grouping (a)–(e) according to Section 3.2. Deviations from a general increasing trend (1) occur in both directions (2 and 3); for explanations see text. Horizontal error bars represent the standard deviation ($1\sigma$) of the porosity distributions. Uncertainties in VEI are depicted by vertical error bars.

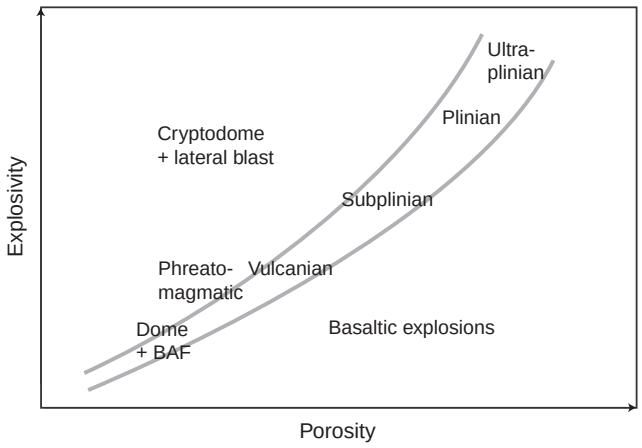


**Fig. 4.** Generalized correlation between porosity, explosivity, and eruptive characteristics.

Similarly, phreatomagmatic explosions show a slightly higher explosivity than expected on the basis of their mean porosity. As outlined in Section 3.1, this can be explained by the fact that (i) the magma–water interaction provides extra energy, which helps to erupt relatively dense magma, (ii) the quenching of the magma due to the contact with water suppresses further vesiculation, and (iii) potentially dense country-rock fragments in the deposit may reduce its overall porosity.

Integration of the main eruptive characteristics into the trends shown in Fig. 3, we propose a generalized schematic diagram correlating porosity, explosivity and eruption type (Fig. 4). The main trend follows the eruption styles of intermediate to high silica volcanoes: dome building–Vulcanian–Subplinian–Plinian–Ultraplinian. Low-viscosity basaltic eruptions fall below the trend, eruptions hindered by confinement (cryptodome growth), above the trend.

The trends described here are based on certain simplifications that should be considered in the interpretation of porosity distributions. Firstly, the value of mean porosity loses some relevance as data distributions get more complex, e.g., bimodal or strongly skewed. Secondly, one has to take into account that the datasets of density and porosity data interpreted in this work differ in size, quality and density determination method. This may cause uncertainties within the absolute values of the statistical parameters. Thirdly, the VEI is of necessity an incomplete parameterisation of the explosivity of an eruption. It is mainly based on an estimated erupted bulk volume of a single eruptive event and does not account for the deposit's density. The density of tephra deposits may vary considerably, meaning that two eruptions with a comparable mass of erupted magma may produce bulk tephra deposits of quite different volumes and thus different VEI measures. Furthermore, the consideration of only the volume of erupted material does not provide information on the intensity of an eruption, i.e. the mass eruption rate (Mason et al., 2004, Pyle, 1995). However, VEI is frequently used, and inasmuch useful as a comparative index, as plenty of data on tephra volume are available in online databases. The more significant pair of indices $M$ (eruption mass) and $I$ (eruption intensity), as proposed by Pyle, 1995, often suffer from the lack of underlying data.

## 5. Summary

We have analysed the porosity distributions of deposits of 17 different eruptions. According to characteristic parameters such as mean porosity, variance, modality and skewness, we categorize the distribution diagrams into five groups, corresponding to the fragmentation- and eruption styles dome forming, explosive basaltic, cryptodome forming, Subplinian–Plinian–Ultraplinian, and phreatomagmatic. We find that the mean porosity values of the deposits show a general, slightly non-linearly increasing correlation with the Volcanic Explosivity Index (VEI). Efficient degassing, either due to a low magma viscosity or to an effective permeable network, leads to a decrease of the explosivity of an eruption. Hence we find that basaltic explosive activity plots below the general trend. In contrast, permeable degassing and stress relaxation are hindered in cryptodome-forming eruptions, which cause overpressure to build up in the system. Indeed, these eruptions are characterized by low porosity material and high explosivity, leaving these eruptions above the trend with high VEI. In phreatomagmatic explosions, the vesiculation process is interrupted by the magma-water contact, resulting in a slightly lower-than-expected porosity.

The described categorization of porosity distributions, as well as the correlation between porosities of pyroclastic deposits and VEI, add useful tools in the interpretation of pyroclastic deposits where no records of eruption characteristics are available. In combination with other criteria, a sufficiently large database of porosity distributions might help to characterize eruption styles of an entire eruption or single eruption phases. With an extension of the database, it might be further possible to unravel more complex, multimodal distributions and link the components to different eruption styles and phases.

## Acknowledgements

The thorough reviews of Gill Jolly and an anonymous reviewer helped to improve the manuscript. We thank Yan Lavallée, whose contributions and ideas helped to improve the paper, and Simon Kremers for his assistance during field work. This is publication No. GEOTECH-1528 of the R&D Programme GEOTECHNOLOGIEN funded by the German Ministry of Education and Research (BMBF) and German Research Foundation (DFG), Grant PTJ MGS/03G584A-SUNDAARC-DEVACOM.

## Appendix A. Supplementary data

Supplementary data to this article can be found online at doi:10.1016/j.jvolgeores.2011.04.006.

## References

Adams, N.K., Houghton, B.F., Hildreth, W., 2006. Abrupt transitions during sustained explosive eruptions: examples from the 1912 eruption of Novarupta. Alaska. Bull. Volcanol. 69, 189–206.
Alidibirov, M., Dingwell, D.B., 1996. Magma fragmentation by rapid decompression. Nature 380, 146–148.
Bagdassarov, N., Dingwell, D.B., 1994. Thermal properties of vesicular rhyolite. J Volcanol. Geotherm. Res. 60, 179–191.
Belousov, A., Belousova, M., 2001. Eruptive process, effects and deposits of the 1996 and the ancient basaltic phreatomagmatic eruptions in Karymskoye lake, Kamtchatka, Russia. Spec. Publ. Int. Assoc. Sediment. 30, 35–60.
Belousov, A., Voight, B., Belousova, M., 2007. Directed blasts and blast-generated pyroclastic density currents: a comparison of the Bezymianny 1956, Mount St Helens 1980, and Soufrière Hills, Montserrat 1997 eruptions and deposits. Bull. Volcanol. 69, 701–740.
Cashman, K.V., Sturtervant, B., Papale, P., Navon, O., 2000. Magmatic fragmentation. In: Sigurdsson, H. (Ed.), Encyclopedia of Volcanoes. Academic Press, London, pp. 421–430.
Eichelberger, J.C., Carrigan, C.R., Westrich, H.R., Price, R.H., 1986. Non-explosive silicic volcanism. Nature 323, 598–602.
Fowler, A.C., Scheu, B., Lee, W.T., McGuinness, M.J., 2010. A theoretical model of the explosive fragmentation of vesicular magma. Proc. R. Soc. London, Ser. A 466, 731–752.
Hoblitt, R.P., Harmon, R.S., 1993. Bimodal density distribution of cryptodome dacite from the 1980 Eruption of Mount St. Helens, Washington. Bull. Volcanol. 55, 421–437.
Houghton, B.F., Smith, R.T., 1993. Recycling of magmatic clasts during explosive eruptions: estimating the true juvenile content of phreatomagmatic volcanic deposits. Bull. Volcanol. 55, 414–420.
Houghton, B.F., Wilson, C.J.N., 1989. A vesicularity index for pyroclastic deposits. Bull. Volcanol. 51, 451–462.
Houghton, B.F., Wilson, C.J.N., Rosenberg, M.D., Smith, I.E.M., Parker, R.J., 1996. Mixed deposits of complex magmatic and phreatomagmatic volcanism: an example from Crater Hill, Auckland, New Zealand. Bull. Volcanol. 58, 59–66.

Kueppers, U., Scheu, B., Spieler, O., Dingwell, D.B., 2005. Field-based density measurements as tool to identify pre-eruption dome structure: set-up and first results from Unzen volcano, Japan. J. Volcanol. Geotherm. Res. 141, 65–75.
Lautze, N.C., Houghton, B.F., 2008. Single explosions at Stromboli in 2002: use of clast microtextures to map physical diversity across a fragmentation zone. J. Volcanol. Geotherm. Res. 170, 262–268.
Llewellin, E.W., Mader, H.M., Simpson, S.D.R., 2002. The rheology of a bubbly liquid. Proc. R. Soc. London, Ser. A 458, 987–1016.
Mason, B.G., Pyle, D.M., Oppenheimer, C., 2004. The size and frequency of the largest explosive eruptions on Earth. Bull. Volcanol. 66, 735–748.
Mueller, S., Melnik, O., Spieler, O., Scheu, B., Dingwell, D.B., 2005. Permeability and degassing of dome lavas undergoing rapid decompression: an experimental determination. Bull. Volcanol. 67, 526–538.
Mueller, S., Scheu, B., Spieler, O., Dingwell, D.B., 2008. Permeability control on magma fragmentation. Geology 36, 399–402.
Newhall, C.G., Self, S., 1982. The volcanic explosivity index (VEI): an estimate of explosive magnitude for historical volcanism. J. Geophys. Res. 87, 1231–1238.
Polacci, M., Pioli, L., Rosi, M., 2003. The Plinian phase of the Campanian ignimbrite eruption (Phlegrean Fields, Italy): evidence from density measurements and textural characterization of pumice. Bull. Volcanol. 65, 418–432.
Pyle, D.M., 1995. Mass and energy budgets of explosive volcanic eruptions. Geophys. Res. Lett. 5, 563–566.
Siebert, L., Simkin, T., 2002. Volcanoes of the World: an Illustrated Catalogue of Holocene Volcanoes and their Eruptions. Smithsonian Institution. Global Volcanism Program Digital Information Series, GVP-3. http://www.volcano.si.edu/world/.
Sparks, R.S.J., 1978. The dynamics of bubble formation and growth in magmas: a review and analysis. J. Volcanol. Geotherm. Res. 3, 1–37.
Spieler, O., Kennedy, B., Kueppers, U., Dingwell, D.B., Scheu, B., Taddeucci, J., 2004. The fragmentation threshold of pyroclastic rocks. Earth Planet. Sci. Lett. 226, 139–148.